

PACS numbers: 42.55.Px; 42.60.Da; 42.65.Sf
DOI: 10.1070/QE2001v031n02ABEH001904

Synchronisation of unidirectionally coupled two-frequency chaotic lasers

A P Napartovich, A G Sukharev

***Abstract*. The nonlinear behaviour of a pair of optically coupled semiconductor laser diodes is studied for different coefficients of optical coupling and different pump currents. As the pump current increases, the behaviour of the system undergoes several transformations from stationary behaviour to a periodic behaviour and then to chaos. Approximate formulas for the self-oscillation frequency of the system and other characteristics of the pair of lasers are derived as functions of the pump current. An analytic expression is found for the critical pump intensity above which there appears a non-zero average difference between the frequencies of the lasers. The behaviour of these regimes in the coupled lasers is characterised by the fixed phase incursion of the fields per period. The chaotic behaviour of two-section semiconductor lasers arranged in the controlling laser – slave laser configuration is studied numerically. The possibility of an almost complete synchronisation of the chaos is demonstrated in this scheme.**

***Keywords*:** *synchronous chaos, two-frequency laser, optical communication.*

1. Introduction

The research interest in the dynamic chaos in various physical systems has been constantly growing recently. As researchers get deeper insight in the complex behaviour of chaotic systems, they develop new control methods and practical applications of chaotic behaviour. In particular, the dynamic chaos can be used for the secure transmission of encoded information through communication channels. For this purpose, one has to obtain lasing in a chaotic mode, control the lasing parameters, and synchronise the chaotic operation of the transmitter and the receiver. It has been established that many laser systems can exhibit dynamic chaos. In particular, there are ways to obtain a chaotic output from semiconductor lasers. The usability of semiconductor lasers for optical communications and the possibility of obtaining chaos in them account for their special role in chaos-based optical cryptography systems.

A concrete scheme of a laser communication channel in which a chaotic signal emitted by a laser transmitter was coded and then transferred to a receiver representing a laser identical to the transmitter, was considered theoretically in Ref. [1] and experimentally realised in Refs [2, 3].

The scheme for coding/decoding information in a chaotic sequence of laser pulses is based on a nontrivial effect: When an optical signal additionally modulated by the information signal is injected into a slave laser, which is identical to the controlling laser, the former removes the modulation and reconstructs the original radiation [1]. Comparing the received information-carrying beam with the output of the slave laser, one can reconstruct the encoded information.

Thus, this scheme features two key processes: (1) The synchronisation of the receiving laser to which a chaotic signal is injected from an identical laser transmitter and (2) The erasure of the information delivered in the injected beam. Various factors can affect the quality of these processes. The influence of the non-equivalence of the laser transmitter and receiver significantly depends on the characteristics of the chaos (in particular, its fractal dimensionality), which, in turn, are determined by the mechanism of the chaos development in the lasers. The scheme under consideration has been studied best for the situation when the chaos was induced by a periodic modulation of the pumping rate. In particular, we have shown earlier [4] that the synchronisation of the chaotic laser that was controlled by the injected chaotic signal from a frequency-detuned controlling laser was incomplete. However, the resulting difference between the fields was small, leaving the possibility of practical applications.

Obviously, the information loss in the receiver that preserves the carrier chaotic radiation does not take place in any circumstances. There are restrictions on the coded information density and the degree of identity of the lasers. We have earlier studied numerically the question about the permissible frequency bandwidth for data communication in the case when the two lasers were identical and the chaos was produced by a periodic pump [5]. We have found that the bandwidth of the information signal should not exceed ~ 0.2 of the relaxation oscillation frequency of the laser.

These studies were performed for a model system of optically coupled CO_2 lasers (with unidirectional coupling). We have noted above that semiconductor lasers are the real candidates for optical cryptography applications. Concerning the lasing behaviour, a novel factor, which was ignored in the systems investigated earlier, is the self-modulation of radiation in semiconductors due to nonlinear refraction, which is mainly determined by the contribution propor-

A P Napartovich, A G Sukharev Troitsk Institute for Innovation and Thermonuclear Research, State Scientific Centre of Russian Federation, 142190 Troitsk, Moscow oblast, Russia

Received 28 August 2000
Kvantovaya Elektronika **31** (2) 147 – 153 (2001)
Translated by I V Bargatin

tional to inversion. A simple way to achieve the chaotic operation regime in a laser diode is to employ a two-section design in which the sections are optically coupled (Fig. 1). As was shown numerically in Ref. [6], at a certain distance between the sections (i.e., at a given optical coupling constant), the laser starts to generate spikes randomly distributed in time. Methods for producing chaos that do not require external fixed-frequency sources for the modulation of the system parameters offer some advantages, especially at high frequencies, which are necessary for increasing the information channel bandwidth. Note also that it is easier to distinguish and decode the data signal in the case of a low-dimensional chaos (according to Lyapunov) than in the case of a high-dimensional one [7].

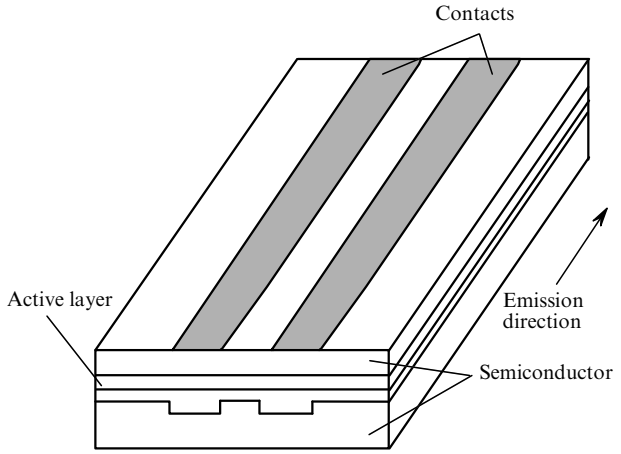

Figure 1. Schematic of the two-emitter laser diode.

The above arguments explain the importance of studying the nonlinear behaviour of two-section laser diodes exhibiting chaos of a higher dimensionality. This problem demands a large amount of calculations, which explains why we use the simple coupled-mode theory. A comparison between our results and those of Ref. [6], in which a pair of optically coupled laser diodes was studied using a model with distributed parameters, demonstrates the identity of the regimes observed.

The purpose of this work was to study analytically and numerically the sequence of the lasing regimes observed with increasing current in the two-section laser diode, to choose chaotic regime of a high dimensionality, and to study numerically the synchronisation of the second pair of the section by injecting radiation of the first pair.

2. Model of two-section laser diode

Fig. 1 shows the schematic of a two-section semiconductor laser that was considered in Ref. [6]. The evolution of the electromagnetic field $E_{1,2}(t)\exp(-\mathrm{i}\omega t)$ inside the two semiconductor laser diodes is described by the truncated wave equations for the slowly varying complex amplitudes [8]:

$$\frac{\partial \mathscr{E}_1}{\partial t} = \frac{1}{2}\left[G(\mathscr{N}_1) - \frac{1}{\tau_{\mathrm{ph}}}\right](1 - \mathrm{i}R)\mathscr{E}_1 + \mathrm{i}\mathscr{M}\mathscr{E}_2, \tag{1}$$

$$\frac{\partial \mathscr{E}_2}{\partial t} = \frac{1}{2}\left[G(\mathscr{N}_2) - \frac{1}{\tau_{\mathrm{ph}}}\right](1 - \mathrm{i}R)\mathscr{E}_2 + \mathrm{i}\mathscr{M}\mathscr{E}_1. \tag{2}$$

Here, $G(\mathscr{N}_{1,2})$ is the probability of induced photon emission (amplification), which depends on the carrier density $\mathscr{N}_{1,2}$; τ_{ph} is the lifetime of cavity photons; $\mathscr{M}$ is the coupling constant between the adjacent lasers; R is the anti-waveguide parameter, also known as the line enhancement factor. The parameter R is proportional to the ratio of the rate of variation in the refractive index η to the rate of variation in the gain G during variation in the carrier density $\mathscr{N}$:

$$R = -2k_0\left(\frac{\partial\eta/\partial\mathscr{N}}{\partial G/\partial\mathscr{N}}\right), \tag{3}$$

where $k_0 = \omega/c$ is the wave number corresponding to the central frequency of the wave mode of the laser. Usually, $\partial\eta/\partial\mathscr{N} < 0$, and an increase in the number of carriers reduces the real part of the refractive index, so that $R > 0$ ($R = 2 - 6$). If the lasing threshold is not greatly exceeded, the gain can be written as $G(\mathscr{N}_{1,2}) = G(\mathscr{N}_{\mathrm{th}}) + (\mathscr{N}_{1,2} - \mathscr{N}_{\mathrm{th}})g$, where $\mathscr{N}_{\mathrm{th}}$ is the threshold carrier density; $G(\mathscr{N}_{\mathrm{th}}) = 1/\tau_{\mathrm{ph}}$; $g = \partial G/\partial\mathscr{N}$ is the differential gain.

The carrier density is determined by the rate equations [9]

$$\frac{\partial \mathscr{N}_{1,2}}{\partial t} = p - \frac{\mathscr{N}_{1,2}}{\tau_{\mathrm{s}}} - G(\mathscr{N}_{1,2})|\mathscr{E}_{1,2}|^2, \tag{4}$$

where p is the intensity of the pump and τ_{s} is the lifetime of carriers. The term $\mathscr{N}_{1,2}/\tau_{\mathrm{s}}$ in equation (4) describes the carrier loss due to spontaneous emission. The loss due to stimulated emission is described by the term containing the squared field amplitude $|\mathscr{E}_{1,2}|^2$.

Let us renormalise the variables:

$$X_{1,2} = \left(\frac{g\tau_{\mathrm{s}}}{2}\right)^{1/2}\mathscr{E}_{1,2}, \quad N_{1,2} = \frac{1}{2}\,g\tau_{\mathrm{ph}}(\mathscr{N}_{1,2} - \mathscr{N}_{\mathrm{th}}),$$

$$P = \frac{1}{2}\,g\tau_{\mathrm{ph}}(p\tau_{\mathrm{s}} - \mathscr{N}_{\mathrm{th}}), \quad T = \frac{\tau_{\mathrm{s}}}{\tau_{\mathrm{ph}}}, \quad \tau = \frac{t}{\tau_{\mathrm{ph}}}, \quad M = \mathscr{M}\tau_{\mathrm{ph}}.$$

Here, $X_{1,2}$ is the normalised field amplitude; $N_{1,2}$ is the normalised excess of the carrier density over the threshold one; P is the normalised excess of the pumping intensity over the threshold one. Equations (1), (2), and (4) then assume the form

$$\frac{\partial X_{1,2}}{\partial\tau} = (1 - \mathrm{i}R)N_{1,2}X_{1,2} + \mathrm{i}MX_{2,1}\,, \tag{5}$$

$$T\,\frac{\partial N_{1,2}}{\partial\tau} = P - N_{1,2} - (1 + 2N_{1,2})|X_{1,2}|^2. \tag{6}$$

The authors of Ref. [6] used the line enhancement factor $R = 3$, the carrier lifetime $\tau_{\mathrm{s}} = 2000$ ps, and the lifetime of the cavity photons $\tau_{\mathrm{p}} = 2.27$ ps for the AlGaAs laser, which yields $T = 881$. In the following, we will use the parameters that are close to these values. To analyse the solutions obtained, it is convenient to pass on to real variables – the amplitude and the phase. By representing the complex fields $X_{1,2}$ as $E_1\exp(\mathrm{i}\varphi_1)$ and $E_2\exp(\mathrm{i}\varphi_2)$ and introducing the phase difference $\varphi = \varphi_2 - \varphi_1$, we obtain the equations

$$\frac{\partial E_1}{\partial\tau} = N_1E_1 - ME_2\sin\varphi\,, \tag{7}$$

$$\frac{\partial E_2}{\partial \tau} = N_2 E_2 + M E_1 \sin\varphi\,, \tag{8}$$

$$\frac{\partial \varphi}{\partial \tau} = R(N_1 - N_2) + M\left(\frac{E_1}{E_2} - \frac{E_2}{E_1}\right)\cos\varphi\,, \tag{9}$$

$$T\frac{\partial N_1}{\partial \tau} = P - N_1 - (1 + 2N_1)E_1^2\,, \tag{10}$$

$$T\frac{\partial N_2}{\partial \tau} = P - N_2 - (1 + 2N_2)E_2^2\,. \tag{11}$$

3. Analytical study of the possible regimes in two-section lasers

By varying the strength of coupling between the lasers in a single pair, the authors of Ref. [6] discovered several bifurcations, initially leading to regular pulsations and then, via a series of period doublings, to chaos. To determine explicitly the parameter regions where one or other regime is observed, we performed an approximate analysis based on the numerical solution of system (7)–(11). We varied the pump intensity P, which was related to the current through the diode, and the coupling constant M. For definiteness, we chose the normalised relaxation time $T = \tau_s/\tau_p$ of the carriers to be 1000 and the line enhancement factor to be $R = 3$. For the fixed value of M, a variation in the pump current changes the lasing dynamics of the two-section laser.

Equations (7)–(11) have two stationary solutions: $E_1^2 = E_2^2 = P$, $N_1 = N_2 = 0$, $\varphi = 0$ and π. By linearising the system of equations near a stationary solution, we can determine its stability to small perturbations of the fields e_1 and e_2, of the phase $\tilde{\varphi}$, and of the carrier concentrations n_1 and n_2. The matrix of the system of the five linear equations can be transformed to a $3 \otimes 2$ block-diagonal matrix in the basis of variables $(e_2 - e_1)$, $\tilde{\varphi}$, $(n_2 - n_1)$ plus $(e_1 + e_2)$, $(n_1 + n_2)$. The eigenvalues, which determine the development of instabilities, are the roots of the third-order characteristic polynomial (in the two-dimensional subspace, the stationary solutions are stable):

$$\sum_{j=0}^{3} a_j \lambda^{3-j} = 0,$$

where

$$a_0 = 1;\ a_1 = \frac{1 + 2P}{T};\ a_2 = \frac{2P}{T} + 4M^2\cos^2\varphi;$$

$$a_3 = \frac{1 + 2P}{T}\,4M^2\cos^2\varphi - \frac{2PR}{T}\,2M\cos\varphi.$$

According to the Routh–Hurwitz criterion, the system is stable if $a_3 > 0$ and $a_1 a_2 - a_0 a_3 > 0$. These conditions are different for the inphase and antiphase solutions [10]. The inphase solution $\varphi = 0$ is stable at

$$M > \frac{PR}{1 + 2P}. \tag{12}$$

The loss of stability is due to aperiodic growth of perturbations. The antiphase solution $\varphi = \pi$ is stable at

$$M < \frac{1 + 2P}{2TR}. \tag{13}$$

In the latter case, the loss of stability results in oscillations at the frequency $\Omega = (2P/T + 4M^2)^{1/2}$.

For the chosen values $T = 1000$ and $R = 3$, the antiphase solution becomes unstable at very weak coupling between the channels. For this reason, it is more interesting to study the evolution of the inphase solution from a stationary solution to self-oscillations. According to inequality (12), the critical pump intensity is of the order of the coupling constant: $P \sim M/R$. Note that, for the coupled-mode theory to be applicable, we need $M \ll 1$. Thus, we can restrict ourselves to studying the region where $P \ll 1$.

We found that upon crossing the stability boundary (12), a stationary solution appears, which corresponds to different field intensities E_1^2 and E_2^2 (spontaneous symmetry breakdown), related by the expression

$$\frac{E_1^2 - E_2^2}{E_1^2 + E_2^2} = -\left[\frac{PR}{M} - (1 + 2P)\right]^{1/2}. \tag{14}$$

Simultaneously, a phase difference of the same order of magnitude appears between the fields:

$$\varphi \approx \frac{1}{R}\left[\frac{PR}{M} - (1 + 2P)\right]^{1/2}. \tag{15}$$

As the pump intensity increases up to

$$P > \frac{M}{R}\left(1 + \frac{2M}{R} + \frac{R}{4MT}\right) \tag{16}$$

the nonsymmetric solution also becomes unstable and leads to self-oscillations.

For the further analysis of the self-oscillation regimes, it is convenient to perform another transformation of the equations. We can treat the amplitudes $E_1 > 0$ and $E_2 > 0$ of the fields, as projections of the total field $E = (E_1^2 + E_2^2)^{1/2}$ on two axes. In this case, we can change over to the polar system of coordinates (the radius vector and the angle). Equations (7)–(11) assume a simpler form if we introduce the total power $\rho = E_1^2 + E_2^2$, the double angle ψ satisfying $\sin\psi = 2E_1E_2/\rho > 0$ and $\cos\psi = (E_1^2 - E_2^2)/\rho$, and make the following change of variables for the carrier concentrations: $2N = N_1 - N_2$ and $2n = N_1 + N_2$. Renormalising the time once again ($\tau_M = 2M\tau$), we obtain the system of equations

$$\dot{\rho} = \frac{\rho N}{M}\left(\cos\psi + \frac{n}{N}\right), \tag{17}$$

$$\dot{\varphi} = R\,\frac{N}{M} + \frac{\cos\psi}{\sin\psi}\cos\varphi, \tag{18}$$

$$\dot{\psi} + \frac{N}{M}\sin\psi = \sin\varphi, \tag{19}$$

$$4MT\dot{N} = -2N(1 + \rho) - (1 + 2n)\rho\cos\psi, \tag{20}$$

$$4MT\dot{n} = 2P - 2n - \rho(1 + 2n + 2N\cos\psi), \tag{21}$$

where the dot denotes the derivative with respect to the time τ_M.

Obviously, ρ has the meaning of the total laser output power; the angle ψ, lying within the first quadrant, characterises the difference between the output powers of the lasers; $2n$ is the average inversion; and $2N$ is the difference between the inversions in the sections. Fig. 2 shows a typical calculated shape of the periodic self-oscillations (similar self-oscillations were also studied in Ref. [6]). Figs 3–5 show the temporal behaviour of above quantities.

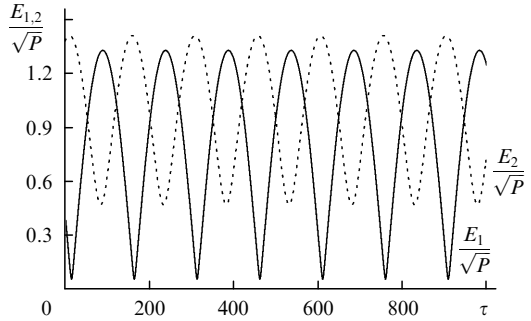

Figure 2. Time dependences of the field amplitudes E_1 and E_2 for $P = 0.02$ and $M = 0.02$.

The conclusions we can draw from Figs 3–5 allow us to analyse approximately the bifurcations of the solutions. The quantity $\kappa = M(1+2P)/PR \approx M/PR$, which equals unity in the point of the spontaneous symmetry breakdown, will serve as the controlling parameter. For a given coupling constant M, κ decreases with increasing pumping intensity, giving rise to self-oscillations which change with the further reduction in κ. In Figs 2–5, the parameter $\kappa \approx 0.35$. The variation in the phase difference remains finite but increases with decreasing κ.

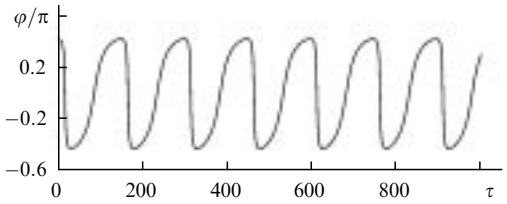

Figure 3. Time evolution of the frequency difference φ between the sections for $P = 0.02$ and $M = 0.02$.

The total laser power (Fig. 4) is almost constant, whereas the difference between the field intensities varies greatly. Note that the average inversion always remains close to zero (Fig. 5), while the difference between the inversions slightly oscillates near a positive value. (This means that the first laser is always in the above-threshold regime, whereas the second laser is always in the below-threshold regime, $N_2 < 0$). Thus, the spontaneous symmetry breakdown is also preserved in the self-oscillation regime. Based on the calculation results shown in Figs 3–5, we can write down a useful system of inequalities:

$$n \ll N \ll P \ll 1. \tag{22}$$

In addition, it follows from Fig. 5 that $N/M \ll 1$.

Our numerical calculations (see also Ref. [6]) have shown that another bifurcation occurs with increasing

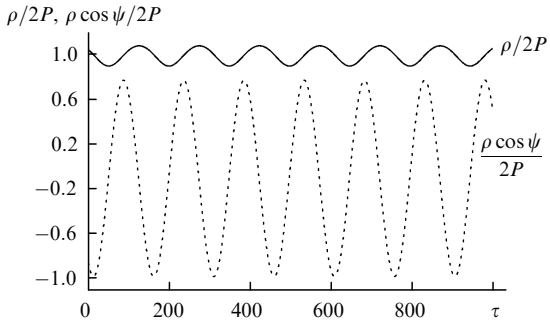

Figure 4. Time dependences of the total power ρ and the power difference $\rho\cos\psi$ for $P = 0.02$ and $M = 0.02$.

pump intensity, after which the phase difference between the fields begins to grow infinitely, corresponding to the appearance of a finite (nonzero) average frequency difference. The main purpose of our analysis is to find the critical parameters at which this bifurcation occurs.

One can see from Figs 3–5 that the degrees of modulation of the total power ρ and the inversion difference $2N$

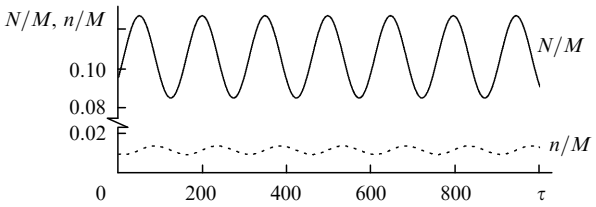

Figure 5. Time evolution of the half-sum n and the half-difference N between the inversions for $P = 0.02$ and $M = 0.02$.

are small with respect to their average values. The latter can be related by averaging equations (17), (20), and (21) over one period:

$$\bar{\rho} = 2(P - \bar{n}) \approx 2P, \tag{23}$$

$$\overline{\cos\psi} = -\frac{\bar{N}}{P} = -\frac{\bar{n}}{\bar{N}}. \tag{24}$$

Thus, the relative average power difference $|\overline{\cos\psi}|$ (the bar denotes averaging over the period) plays the role of a small parameter for the system of inequalities (22). The further calculations are rather involved; therefore, we will omit them and present directly the final approximate relations, which provide a complete parametric description of the behaviour of the system of two lasers. The approximate analysis allows us to obtain the dependence of the average inversion difference on the pump intensity,

$$\bar{N} \simeq \left(\frac{P}{4T}\right)^{1/2}, \tag{25}$$

and to determine the average power difference $\overline{\cos\psi} = -(4PT)^{-1/2}$ from equation (24).

In addition, one can show that the combination

$$C = \sin\psi\cos\varphi - R\frac{N}{M}\cos\psi \tag{26}$$

also varies very little with time, whereas the variations of its individual terms are much larger than the corresponding average values. Assuming $C = \text{const}$, eliminating $\cos\varphi$ from relation (26), and using equation (19) and the smallness of the ratio N/M, we can derive the equation for $\cos\psi$, which turns out to be the Newton equation for the motion in a parabolic potential and can easily be solved. The solution of this equation yields the explicit expression for the self-oscillation frequency Ω:

$$\Omega = \left(1 + \frac{R^2P}{4M^2T}\right)^{1/2}. \tag{27}$$

This solution also yields another relation for the relative average population inversion: $\overline{\cos\psi} \approx -CR\bar{N}/M$. Comparing it to relation (24), we obtain the expression for the average C:

$$C \approx \frac{M}{RP} = \kappa. \tag{28}$$

Our numerical calculations show that, as the pump intensity increases, the phase difference begins to grow indefinitely at some moment, corresponding to the appearance of a nonzero average frequency difference between the fields. On the phase diagram in coordinates φ and ψ, this phenomenon appears as the transformation of the closed curve shown in Fig. 6 (the limiting cycle) to the open curve (shown in Fig. 7) accompanied by a change in the φ by 2π. The critical point of this transformation corresponds to the vanishing of $\cos\varphi$, i.e., to the condition $C = C_{\text{cr}} \simeq R\bar{N}/M$ (one can see from Fig. 6 that $\cos\psi \approx -1$ when the limiting cycle opens). Using expressions (25) and (28), we find the critical pump intensity

$$P_{\text{cr}} \simeq \frac{M}{R}\left(\frac{4TM}{R}\right)^{1/3}. \tag{29}$$

Note that expression (27) for the self-oscillation frequency also agrees with the numerical results obtained for the pump intensity above the threshold.

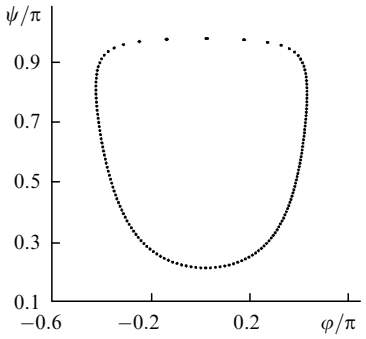

Figure 6. Phase portrait $\psi(\varphi)$ for $P = 0.02$ and $M = 0.02$.

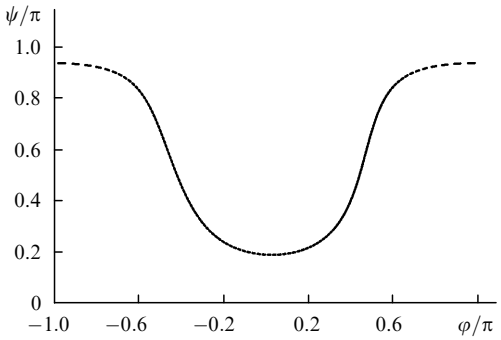

Figure 7. Phase portrait $\psi(\varphi)$ for $P = 0.04$ and $M = 0.02$.

4. Numerical results

4.1 Dynamics of the two-section laser

We solved equations (7)–(11) numerically for several values of $M \ll 1$ and various pump intensities P. In this discussion, we will restrict ourselves to the case of $M = 0.02$. According to (12), at $P < 0.0068$ the two-emitter laser operates in the stationary regime, with the output intensities of the both sections being equal. At $P = 0.007$, there is a stationary solution but the output intensities of the two channels differ already. With a good accuracy, the differences between the intensities and the phases are described by expressions (14) and (15). At $P > 0.007$, the stationary nonsymmetric solution becomes unstable and transforms to regular pulsations, also in agreement with the theoretical estimate (16).

Analytic expressions for the frequency of self-oscillations (27) and the average total power (23) agree well with the numerical results. (Note that the normalised times τ_M in expression (27) and in Figs 2–5, τ, differ by factor of $2M$). We also observed the numerical results to agree well with the expressions for the average relative power difference $\overline{\cos\psi}$, the average inversion difference, and the average inversions in the sections (see (24) and (25)). According to the numerical calculations, the degree of modulation of the total output power ρ is 9.2 % ($\sim \bar{N}/M$) (Fig. 4), of the average inversion is 17.7 % ($\sim 2\bar{N}PM^{-2}$) (Fig. 5), and of the average inversion difference is 20 % ($\sim 2\bar{N}/M$) (Fig. 5).

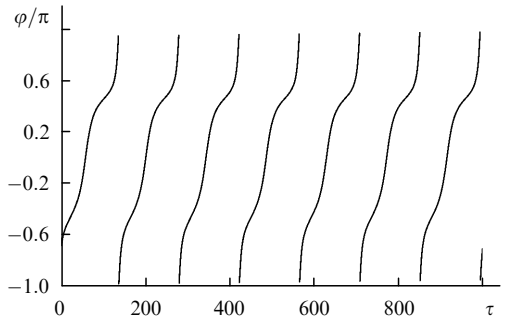

Figure 8. Time evolution of the phase difference φ (in modulus 2π) between the fields of the sections for $P = 0.04$ and $M = 0.02$.

Upon crossing the critical point, the behaviour of the phase difference changes dramatically, as shown in Figs 3, 6–8. Note that the phase difference varies exactly by 2π per

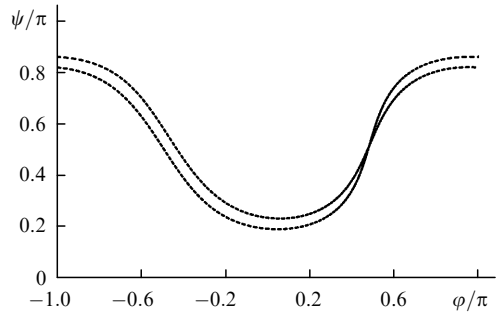

Figure 9. Phase portrait $\psi(\varphi)$ for $P = 0.14$ and $M = 0.02$.

period, preserving the coherence of the interaction between the fields, despite the difference between their average frequencies. According to (29), the bifurcation to a two-frequency periodic solution occurs at $P = 0.022$. Calculations performed for $P = 0.022$ yielded the phase-difference oscillations less than $\pi/2$, whereas at $P = 0.025$, φ increased indefinitely. The further increase in P to 0.14 doubles the period, as shown in Figs 9 and 10 for the dependences $\psi(\varphi)$ and $E_2(E_1)$. In this case, the phase incursion per period is 4π. The period quadruples at $P = 0.154$, and the chaotic lasing begins at $P = 0.159$. Note that the number of positive Lyapunov exponents changes abruptly from zero to two, whereas in the case of a periodic pump, only one exponent becomes positive [5]. Figs 11 and 12 show the chaotic lasing regime at $P = 0.2$. Thus, the dimensionality of the chaos in the system considered is approximately two times greater than in the case of a periodic pump.

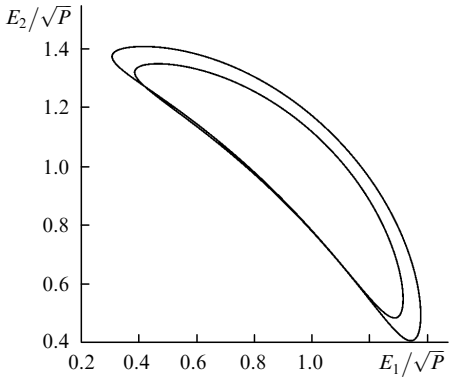

Figure 10. Phase portrait $E_2(E_1)$ for $P = 0.14$ and $M = 0.02$.

4.2 Configuration with the signal injection from one two-section laser to another

We studied the synchronisation of the chaotic two-section lasers experiencing unidirectional coupling (injection) by solving numerically equations (7)–(11) for the controlling laser (sections 1 and 2) and the equations for the slave semiconductor laser (sections 3 and 4, $\varphi_{42} = \varphi_{43} - \varphi + \varphi_{31}$)

$$\frac{\partial E_3}{\partial \tau} = N_3 E_3 - M E_4 \sin\varphi_{43} + K E_1 \sin\varphi_{31}, \tag{30}$$

$$\frac{\partial E_4}{\partial \tau} = N_4 E_4 + M E_3 \sin\varphi_{43} + K E_2 \sin\varphi_{42}, \tag{31}$$

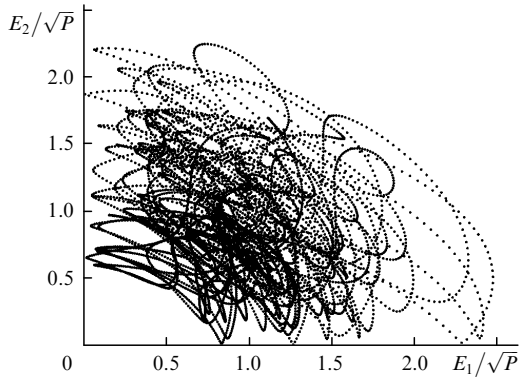

Figure 11. Phase portrait $E_2(E_1)$ for $P = 0.2$ and $M = 0.02$.

$$\frac{\partial \varphi_{43}}{\partial \tau} = R(N_3 - N_4) + M\left(\frac{E_3}{E_4} - \frac{E_4}{E_3}\right)\cos\varphi_{43} + K\left(\frac{E_2}{E_4}\cos\varphi_{42} - \frac{E_1}{E_3}\cos\varphi_{31}\right), \tag{32}$$

$$\frac{\partial \varphi_{31}}{\partial \tau} = R(N_1 - N_3) + M\left(\frac{E_4}{E_3}\cos\varphi_{43} - \frac{E_2}{E_1}\cos\varphi\right) + K\left(\frac{E_1}{E_3}\cos\varphi_{31} - 1\right), \tag{33}$$

$$T\frac{\partial N_3}{\partial \tau} = P - N_3 - (1 + 2N_3)E_3^2, \tag{34}$$

$$T\frac{\partial N_4}{\partial \tau} = P - N_4 - (1 + 2N_4)E_4^2. \tag{35}$$

Here, E_i are the field amplitudes; φ_{ij} is a difference between the phases φ_i of the fields; the coupling constant K describes the radiation injection from section 1 to section 3 and from section 2 to section 4. Equations for the inversion in the slave laser coincide with equations (10) and (11) up to the subscript replacement.

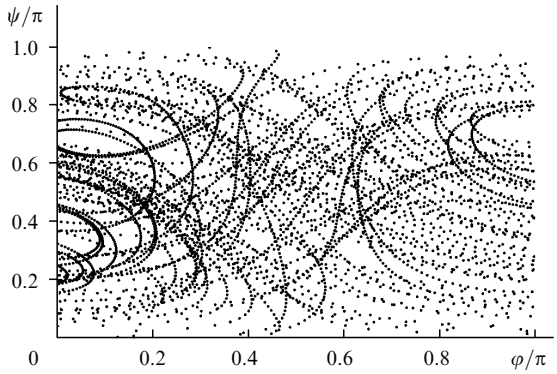

Figure 12. Phase portrait $\psi(\varphi)$ for $P = 0.2$ and $M = 0.02$.

We studied the synchronisation of the two laser pairs operating in the chaotic regime by varying the constant K of the unidirectional coupling for fixed $M = 0.02$ and $P = 0.2$. The controlling laser operated in the chaotic regime (see Figs 11 and 12) with two positive and three negative Lyapunov exponents. The entire system of the two two-section

lasers is described by 11 variables. The resulting space of the Lyapunov exponents has the dimensionality 11, and the number of positive exponents in the chaotic lasing regime is determined by the coupling constant. At $K = 0.01$, there are four positive exponents, at $K = 0.02$ there are three, and at $K = 0.03$ and higher, only two positive exponents remain.

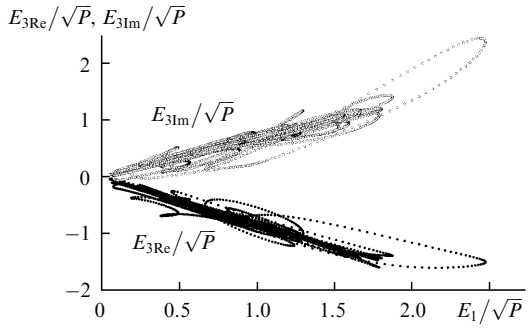

Figure 13. Phase portraits of the real $[E_{3\mathrm{Re}}(E_1)]$ and imaginary $[E_{3\mathrm{Im}}(E_1)]$ parts of the complex field $[E_3 \exp(\mathrm{i}\varphi_{31})]$ for $P = 0.2$, $M = 0.02$, $K = 0.04$.

Since the number of positive Lyapunov exponents of the controlling laser is independent of K and equal to two, the synchronisation of the lasers can take place at $K \geqslant 0.03$. The coupling constant in Figs 13 and 14 is $K = 0.04$. One can see from Fig. 12 that the fields in the two sections of the controlling laser on average oscillate at different frequencies. Nevertheless, the pairs of sections of different lasers (1–3, 2–4) become synchronised. Fig. 13 shows the dependence of the real and imaginary parts of the field $E_3 \exp(\mathrm{i}\varphi_{31})$ on E_1. One can see that the variation is localised in narrow regions along two straight lines. Fig. 14 shows the time dependence of these field amplitudes, demonstrating their strong correlation. In this case, the phase difference φ of the controlling laser and the phase difference φ_{43} of the controlled laser are virtually equal: $\overline{\varphi - \varphi_{43}} = 0$ with a root-mean-square variance of 0.14.

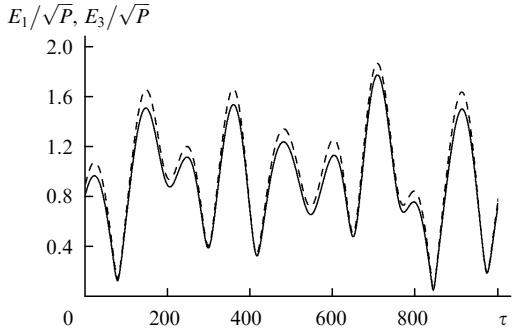

Figure 14. Dynamics of the field amplitudes of the controlling $[E_1(\tau)$, solid curve] and slave $[E_3(\tau)$, dashed curve] lasers for $P = 0.2$, $M = 0.02$, $K = 0.04$.

5. Conclusions

The investigation of the chaos synchronisation calls for a detailed study of the behaviour of a single semiconductor laser operating in various regimes. For the regime of periodic oscillations, we have derived analytic expressions for the frequency of the self-oscillations and for the threshold pump intensity, at which the transition to two-frequency periodic regimes takes place. We have determined the parameter regions where the doubling and quadrupling of the period occurs, as well as the regions of chaotic lasing of a single two-section laser. We have studied the synchronisation of two two-section chaotic lasers in the controlling laser-slave laser configuration. Our numerical analysis has demonstrated the appearance of an incomplete chaos synchronisation at a certain strength of optical coupling between the lasers. The possibility of utilising partially synchronised chaos for secure data communication requires further investigation.

Acknowledgements. The authors thank V N Troshchieva for her help in preparing the figures. This work was supported by the Russian Foundation for Basic Research (Grant No. 98-02-17096).

References

1. Colet P, Roy R *Opt. Lett.* **19** 2056 (1994)
2. van Wiggeren G D, Roy R *Science* **279** 1198 (1998)
3. Goedgebuer J P, Larger L, Porte H Phys. *Rev. Lett.* **80** 2249 (1998)
4. Napartovich A P, Sukharev A G *Zh. Eksp. Teor. Fiz.* **115** 1593 (1999) [*JETP* **88** 875 (1999)]
5. Napartovich A P, Sukharev A G *Kvantovaya Elektron.* **25** 85 (1998) [*Quantum Electron.* **28** 81 (1998)]
6. Rahman L, Winful H G *IEEE J. Quantum Electron.* **30** 1405 (1994)
7. Larger L, Goedgebuer J P, Delorme F *Phys. Rev. E* **57** 6618 (1998)
8. Winful H G, Rahman L *Phys. Rev. Lett.* **65** 1575 (1990)
9. Agrawal G P, Dutta N K *Semiconductor Lasers* (New York: van Nostrand Reinhold, 1993)
10. Winful H G, Wang S S *Phys. Rev. Lett.* **53** 1894 (1988)